COMPARISON OF ALGORITHMS FOR 2D ANISOTROPIC PERMEABILITY CALCULATION IN TERMS OF UNCERTAINTY PROPAGATION

E. Fauster[a*], H. Grössing[b], R. Schledjewski[a,b]

[a]*Chair of Processing of Composites, Department Polymer Engineering and Science, Montanuniversität Leoben, Leoben, Austria*
[b]*Christian Doppler Laboratory for High Efficient Composite Processing, Montanuniversität Leoben, Leoben, Austria*
**ewald.fauster@unileoben.ac.at*

Keywords: liquid composite molding, optical 2-dimensional permeability measurement, computer vision, statistical uncertainty analysis.

Abstract
In this work, a two-dimensional optical permeability measurement system is analyzed with respect to the statistical uncertainty associated with the permeability values. The optical system as well as stochastic material properties and experimental parameters are incorporated in the analysis. Two well-known mathematical algorithms are compared by studying the influence of the individual stochastic parameters on the permeability values. For that purpose, artificially created sets of noisy data have been created and Monte-Carlo experiments have been carried out. The results obtained are finally compared.

1. Introduction

In liquid composite molding (LCM) techniques, dry preforms of reinforcing fabrics are placed in a mold and then impregnated with the liquid polymer matrix material. The impregnation process plays a key role as insufficiently saturated regions directly affect the mechanical properties of the final component. In order to avoid elaborate and expensive impregnation trials, filling simulations can be accomplished. These simulations strongly rely on accurate and trustworthy permeability values.

A well-known approach to determine 2-dimensional permeability values of reinforcing fabrics is based on optical observations of radial flow experiments as introduced by Adams et al. [1]. There, a three-stage procedure has to be followed: (1) acquisition of an image sequence during the actual experiment, whereas the flow front of the saturated fabric shows an elliptic shape in the general case, (2) evaluation of the sequence images to determine the timely advancement of the flow front, i.e. the major and minor axes lengths of an elliptic geometry model approximated to the actual flow front, and (3) calculation of the in-plane permeability values [2] from these characteristics following a specific mathematical algorithm.

Actually, a couple of different algorithms for the computation of the permeability values are reported in the literature. The best known approaches are those of Adams and Rebenfeld [3] on the one hand and Chan and Hwang [4] on the other hand. In this work, a comparison of

these algorithms with respect to their particular impact on the uncertainty of the finally obtained permeability values is presented. Thereby, repeatability analyses following the Monte-Carlo approach are shown. In this sense, this paper represents a continuation of works previously published by the authors [5,6].

2. Basics and Background

2.1. Darcy's Law and the 2D-Permeability Tensor

The process of impregnating a dry preform of reinforcing textiles with liquid matrix material can be understood as saturating a porous structure with a viscous liquid. Following Darcy's law [2], the flow characteristics can mathematically be described according to:

$$\mathrm{v} = -\frac{1}{\eta}\mathrm{K}\nabla\mathrm{p}. \tag{1}$$

Therein, the fluid flow velocity vector $\mathrm{v}\left[\frac{\mathrm{m}}{\mathrm{s}}\right]$ is related with the driving pressure gradient $\nabla\mathrm{p}\left[\frac{\mathrm{N}}{\mathrm{m}^2\,\mathrm{m}}\right]$ through the fluid viscosity $\eta\left[\frac{\mathrm{N\,s}}{\mathrm{m}^2}\right]$ and the permeability of the reinforcing structure, described by the permeability tensor $\mathrm{K}\,[\mathrm{m}^2]$. For planar investigations, the permeability tensor is a $2\,\mathrm{x}\,2$ matrix. By choosing an appropriate coordinate frame (or by application of a coordinate transformation), the primary flow directions can be aligned with the coordinate frame of the measurement system resulting in the simplified tensor:

$$\mathrm{K}_{[2\mathrm{x}2]} = \begin{bmatrix} \mathrm{k_x} & 0 \\ 0 & \mathrm{k_y} \end{bmatrix}, \tag{2}$$

with $\mathrm{k_x}$ and $\mathrm{k_y}$ denoting the permeability values along the primary flow directions.

2.2. Determination of Permeability Values

Basically, permeability measurement is accomplished in a two-step procedure [7]:

1. the actual saturation experiment, i.e. determination of the timely advancement of the fluid impregnating the reinforcing structure, and
2. calculation of the permeability tensor components from these characteristics following a specific mathematical algorithm.

For the calculation of the permeability tensor components by means of the timely characteristics of the flow front advancement, a number of different approaches are reported in the literature. All of these algorithms share the need for finding a solution of the second-order differential equation describing the 2-dimensional pressure distribution $\mathrm{p}(\mathrm{x},\mathrm{y})$ of the fluid impregnating the anisotropic reinforcing structure:

$$\frac{\partial^2\mathrm{p}}{\partial\mathrm{x}^2} + \alpha\frac{\partial^2\mathrm{p}}{\partial\mathrm{y}^2} = 0. \tag{3}$$

Thereby, $\alpha = \frac{\mathrm{k_y}}{\mathrm{k_x}}$ denotes the degree of anisotropy of the reinforcing structure. Adams and Rebenfeld [8] presented an algorithm, which is based on an iterative numerical solution for the degree of anisotropy α. Chan and Hwang [4] on the contrary described an approach which introduces a transformation of the anisotropic problem into an equivalent isotropic system

(EIS). Thereby, the second-order differential equation simplifies to the well-known Laplace equation [2,9,10], for which a closed form solution exists. The resulting isotropic permeability is finally transformed back to the anisotropic system in order to obtain the desired values for k_x and k_y, respectively.

3. Optical Permeability Measurement

3.1. Measurement Principle

The basic principle of the optical permeameter measurement system investigated in this work has originally been presented by Adams et al. [1] and is termed “radial flow experiment”. In Figure 1, a scheme of the setup is shown. The measurement system consists of a mold which is composed of a metal bottom half and a top half built from a glass plate. In between the two halves of the mold, a metal frame with distinct thickness is positioned. The latter component is termed “cavity frame”, as its inner cutting dimensions and thickness specify the mold cavity, i.e. the volume to be filled with the fluid during the experiment.

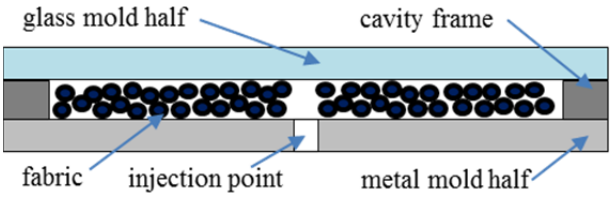

Figure 1: Scheme of an optical permeability measurement system with its major hardware components.

For the actual experiment, layers of the reinforcing textiles are placed inside the cavity, which is subsequently filled with a liquid through a central injection point in the metal bottom half of the mold. During the radial flow experiment, an image sequence is acquired with a camera system positioned above the mold. The camera focusses through the glass plate onto the upper surface of the reinforcing textiles placed inside the cavity. By analysis of the acquired sequence images, the timely advancement of the fluid flow front can be determined.

3.2. The Test Rig

Figure 2 shows a picture of the test rig used for the radial flow experiments in this paper. The frame of the test rig is set up by standard aluminum profiles. Directly on top of the working table, the metal mold half is mounted. The security glass plate forming the upper mold half is made from two glass plates, each with 19 mm in thickness, separated by a 0,76 mm thin polymer foil. The glass mold half is framed with metal profiles in order to connect it to a hinge system on the back side of the test rig. A pneumatic cylinder finally provides for the flapping motion.

The actual mold cavity is specified through the cavity frame showing an inner dimension of 300 mm x 400 mm. After placing the reinforcing structures inside the cavity, the mold is closed by flapping the glass plate into a horizontal position. In addition, the glass plate is tightened with the bottom mold half using a metal clamping frame and a set of screws. The radial flow experiment is then executed by injecting the test fluid into the cavity through a central injection point in the metal bottom mold half. Due to the thickness of the glass plate and the clamping frame used to tighten the glass plate, a maximum injection pressure of 6 bar can be applied.

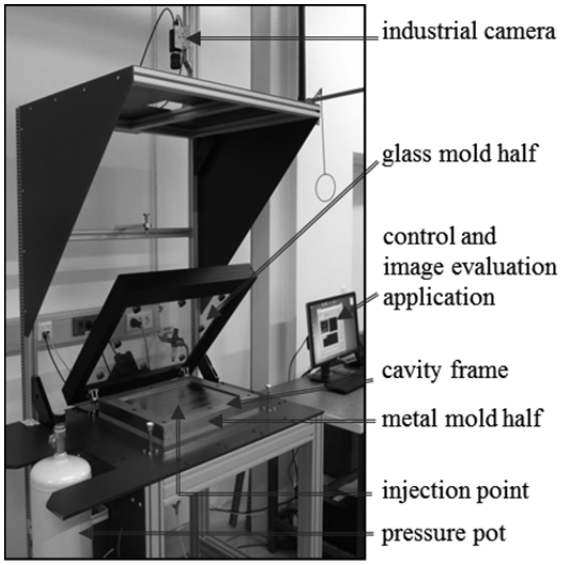

Figure 2: Optical permeability measurement system used for the radial flow experiments.

At a distance of about 1 m above the mold, a camera system consisting of an industrial monochrome camera and a precision lens with a focal length of 16 mm is mounted. The camera is used to acquire an image sequence during the radial flow experiment at an acquisition rate of up to 50 fps at a resolution of 1392 x 1040 pixel. In order to determine the timely advancement of the fluid flow front, the sequence images are evaluated by means of a digital image processing algorithm specifically developed for this application [5]. The algorithm results in an elliptical geometry model (see Figure 3). Thus, the timely flow front advancement is finally obtained in terms of the major and minor axes length characteristics.

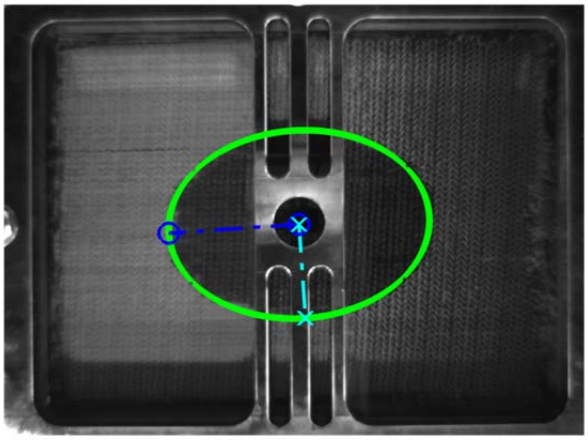

Figure 3: Example of a sequence image with an overlay of the elliptic geometry model fitted to the set of data points found along the fluid flow front.

The test rig control task as well as the image and data acquisition, evaluation and storage tasks have been implemented in a LabVIEW® application. Thereby, the sequence images are evaluated online, i.e. at the same rate as the images are acquired. As a result, the timely flow front advancement is available immediately after finishing the radial flow experiment and the mathematical computation of the permeability tensor components can be accomplished instantaneously.

4. Experimental Work

Permeability values show a significant level of uncertainty with major contributions from inhomogeneities in the reinforcing materials [11,12]. Nonetheless, the measurement system itself also accounts for a certain portion. In order to estimate the contribution of the optical measurement system on the uncertainty associated with the resulting permeability tensor components, a repeatability analysis has been carried out. The analysis is based on a single radial flow experiment. After placing the layers of reinforcing materials inside the mold cavity, the fluid injection has been started together with the acquisition of the image sequence. During the timely advancement of the flow front, the fluid injection has been interrupted at certain stages of the experiment (see Figure 4). However, the acquisition of the image sequence has been pursued and as a result, the radial extent of the elliptic flow front has been acquired virtually at repeatability conditions during these stages of interrupted fluid injection. The fluid injection has been interrupted five times during the experiment and for all of the five sections a number of about 800 images has been acquired and evaluated. The major and minor axes lengths r_x and r_y, have subsequently been analysed by means of Lilliefors tests [13] in order to verify that their statistical nature follows Gaussian probability density functions.

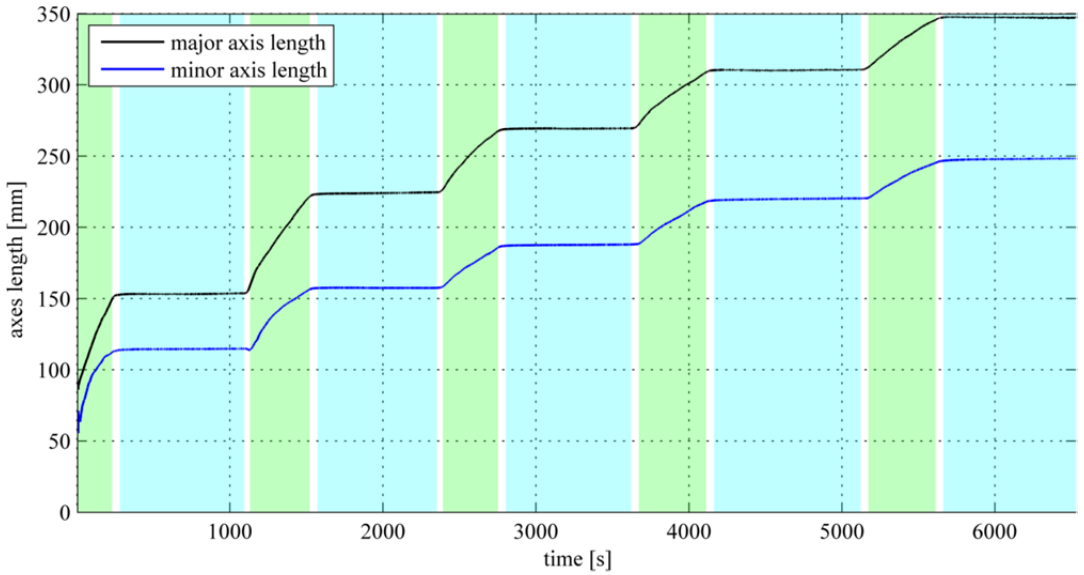

Figure 4: Timely advancement of the flow front in the radial flow experiment with interrupted fluid injection.

The corresponding standard deviation values slightly increase with the flow front extent advancing during the experiment. However, for the uncertainty analysis described in the following section, the standard deviation values have been assumed to be constant over the entire measurement space. Table 1 gives an overview of the incorporated data.

Measurement values	**Symbol**	**Standard dev.**	**Remark**
Major radial extent	r_x	0,175 mm	Results of a statistical analysis as reported by the authors in [5].
Minor radial extent	r_y	0,080 mm	
Time	t	-	The timestamp values representing the image acquisition time are assumed to be deterministic

Table 1: Measurement values obtained for and incorporated in the uncertainty analysis.

5. Uncertainty Analysis

5.1. Parameter Identification

The basis for the uncertainty analysis presented in this paper has been set with the identification of parameters contributing to the uncertainty associated with the permeability values k_x and k_y of an anisotropic reinforcing structure. In Table 2 the experimental parameters incorporated in the analysis are listed.

Experimental parameter	**Symbol**	**Nominal value**	**Standard deviation**	**Remark**
Fluid viscosity	η	65 mPas	0,25% of the nominal value	Precision of the rheological measurement device
Injection pressure	Δp	1,6 bar	1% of the nominal value	Precision of the pressure control valve used in the test rig
Injection radius	r_0	6,5 mm	1% of the nominal value	Estimation based on assumed imperfectness of the machined part
Cavity height	h	5 mm	1% of the nominal value	Estimation based on assumed imperfectness of the machined part

Table 2: Experimental parameters incorporated in the uncertainty analysis.

Moreover, the material of the reinforcing structure - a biaxial non-crimped carbon fibre fabric with polyester stitching yarn - is incorporated in the analysis by means of two uncertain properties as listed in Table 3.

Material properties	**Symbol**	**Nominal value**	**Standard deviation**	**Remark**
Material density (Carbon)	ρ	$1{,}78\ \frac{g}{cm^3}$	1% of the nominal value	Estimation based on assumed imperfectness of the manufacturing process for carbon fibers (chemical impurities)
Areal weight	m_A	$565\ \frac{g}{m^2}$	5% of the nominal value	Uncertainty as stated in data sheet of the biaxial non-crimped carbon fibre fabric

Table 3: Properties of the reinforcing material incorporated in the uncertainty analysis.

5.2. Uncertainty propagation

Following Clarke [14], uncertainty propagation can be addressed either by means of a statistical approach or an analytical approach. The statistical approach - also known as Monte-Carlo experiment - makes use of the law of large numbers [15], i.e. given a sufficiently high number of samples, the covariance can directly be computed using statistical relations.

The uncertainty associated with the material properties and the experimental parameters on the one hand as well as the uncertainty determined for the measurement results of the optical permeameter on the other hand has been propagated to the uncertainty associated with the permeability values k_x and k_y of an anisotropic reinforcing structure. For that purpose, Monte-Carlo experiments have been carried out, i.e. the evaluation algorithms have been executed on $n = 10^4$ artificially created sets of noisy data. In Table 4, the results of the uncertainty analysis are listed for the two evaluation algorithms.

Stochastic parameters						Results of Monte-Carlo experiment (10^4 runs)					
						Chan and Hwang			Adams and Rebenfeld		
Parameter	Symbol	Nominal value		Standard deviation		$\begin{bmatrix}\mu_{k_x}\\ \mu_{k_y}\end{bmatrix}$	$\begin{bmatrix}\sigma_{k_x}\\ \sigma_{k_y}\end{bmatrix}$	σ / μ [%]	$\begin{bmatrix}\mu_{k_x}\\ \mu_{k_y}\end{bmatrix}$	$\begin{bmatrix}\sigma_{k_x}\\ \sigma_{k_y}\end{bmatrix}$	σ / μ [%]
radial extent	r_x r_y	100 .. 350 100 .. 250	mm mm	0,175 0,080	mm mm	1,45E-10 6,44E-11	1,64E-14 1,02E-14	0,01 0,02	1,70E-10 7,61E-11	3,18E-14 9,92E-15	0,02 0,01
density	ρ	1,78	g/cm³	1,00	%	1,45E-10 6,43E-11	1,94E-12 8,58E-13	1,34 1,33	1,70E-10 7,61E-11	1,72E-12 7,69E-13	1,01 1,01
areal weight	m_A	565	g/m²	5,00	%	1,46E-10 6,44E-11	9,60E-12 4,25E-12	6,58 6,60	1,70E-10 7,60E-11	8,48E-12 3,79E-12	4,99 4,99
viscosity	η	65	mPas	0,25	%	1,45E-10 6,44E-11	3,69E-13 1,63E-13	0,25 0,25	1,70E-10 7,60E-11	4,28E-13 1,91E-13	0,25 0,25
injection pressure	Δp	1,6	bar	1,00	%	1,45E-10 6,44E-11	1,44E-12 6,39E-13	0,99 0,99	1,70E-10 7,61E-11	1,71E-12 7,62E-13	1,01 1,00
injection radius	r_0	6,5	mm	1,00	%	1,46E-10 6,44E-11	4,43E-12 1,96E-12	3,03 3,04	1,70E-10 7,61E-11	4,99E-13 2,24E-13	0,29 0,29
cavity height	h	5	mm	1,00	%	1,45E-10 6,43E-11	1,92E-12 8,52E-13	1,32 1,33	1,70E-10 7,61E-11	1,69E-12 7,57E-13	0,99 0,99
all						1,45E-10 6,44E-11	1,10E-11 4,86E-12	7,59 7,55	1,70E-10 7,61E-11	9,01E-12 4,02E-12	5,30 5,28

Table 4: Results of the uncertainty analysis based on Monte-Carlo experiments.

5.1. Comparison of Results

When comparing the average permeability values of k_x and k_y obtained with the two algorithms, a deviation of about 15% can be observed. This is a result of the strongly deviating nature of these two computational algorithms: Adams and Rebenfeld propose an iterative numerical solution for the degree of anisotropy, where Chan and Hwang follow an analytical approach based on an equivalent isotropic system (EIS).

However, the more interesting facets can be discussed when comparing the effects of the individual stochastic parameters on the uncertainty of the permeability values. The results obtained with the algorithm of Adams and Rebenfeld show that the relative uncertainty (i.e. the ratio of standard deviation to nominal value) of the stochastic parameters is directly mapped to the permeability values. This can easily explained as the stochastic parameters contribute linearly to the permeability values. The only exception can be seen for the stochastic injection radius r_0. Given a relative uncertainty of 1% for r_0, a relative uncertainty of about 0.3% is obtained for k_x and k_y. By contrast, the algorithm of Chan and Hwang causes a relative uncertainty for k_x and k_y of about 3% in this situation. This can be explained by the fact that r_0 contributes quadratically to the equivalent isotropic permeability k_{EIS} in their algorithm, thus causing a high sensitivity of the permeability values on r_0.

6. Conclusions

The uncertainty values obtained with the algorithm of Chan and Hwang are consistently higher than the corresponding uncertainty values obtained by the algorithm of Adams and Rebenfeld. This is specifically true for the stochastic injection radius, which is a critical parameter when preparing the preforms for the radial flow experiments. The results obtained in this analysis lead to the proposal to follow the algorithm of Adams and Rebenfeld when computing planar permeability values from the characteristics of the timely flow front advancement in radial flow experiments. However, an extension of this work studying the

systematic deviations of the results obtained with these algorithms is an open issue for future work.

Acknowledgement

The financial support of parts of the work presented by the Austrian Federal Ministry of Economy, Family and Youth is gratefully acknowledged.

References

[1] Adams KL, Russel W, Rebenfeld L. Radial penetration of a viscous liquid into a planar anisotropic porous medium. *International Journal of Multiphase Flow* 1988;14(2):203–15.

[2] Bear J. *Dynamics of fluids in porous media*. New York: Dover; 1988.

[3] Adams KL, Rebenfeld L. Permeability characteristics of multilayer fiber reinforcements. Part I: Experimental observations. *Polym. Compos* 1991;12(3):179–85.

[4] Chan AW, Hwang S. Anisotropic in-plane permeability of fabric media. *Polym. Eng.* Sci. 1991;31(16):1233–9.

[5] Fauster E, Grössing H, Schledjewski R. Uncertainty Analysis for Optical Permeability Measurement of Reinforcing Textiles. In: Proceedings of *ICCM 19*, Montreal, 29.07.-02.08.2013.

[6] Fauster E, Grössing H, Schledjewski R. Statistical Uncertainty Analysis of Material and Measurement Parameters for Optical Permeability Determination. In: Proceedings of *TexComp 2013*, Leuven, Belgium, 2013.

[7] Neitzel M, Mitschang P (Editors). *Handbuch Verbundwerkstoffe: Werkstoffe, Verarbeitung, Anwendung*. München: Hanser; 2004.

[8] Adams KL, Rebenfeld L. In-Plane Flow of Fluids in Fabrics: Structure/Flow Characterization. *Textile Research Journal* 1987;57(11):647–54.

[9] Weitzenböck J, Shenoi R, Wilson P. Measurement of three-dimensional permeability. *Composites Part A: Applied Science and Manufacturing* 1998(29A):159–69.

[10] Weitzenböck J, Shenoi R, Wilson P. Radial flow permeability measurement. Part A: Theory. *Composites Part A: Applied Science and Manufacturing* 1999;30(6):781–96.

[11] Rieber G. Einfluss von textilen Parametern auf die Permeabilität von Multifilamentgeweben für Faserverbundkunststoffe. Kaiserslautern: IVW; 2011.

[12] Grössing H, Wohlfahrt M, Müller A, Schledjewski R. Comparison of Permeability Measurements of Several Fibre Textiles Using Different Measurement Methods. In: Proceedings of *The 15th European Conference on Composite Materials*, Venice, Italy, 2012.

[13] Sachs L. *Angewandte Statistik: Anwendung statistischer Methoden*; mit 317 Tabellen und 98 Übersichten. 8th ed. Berlin, Heidelberg [u.a.]: Springer; 1997.

[14] J. C. Clarke. Modelling Uncertainty: A Primer. Oxford; 1998.

[15] Criminisi A. Modelling and Using Uncertainties in Video Metrology: Oxford; 1997.